# Circularly Permuted $\beta$-Lactamase from *Staphylococcus aureus* PC1[†,‡]

Ursula Pieper, Koto Hayakawa, Zhong Li, and Osnat Herzberg*

*Center for Advanced Research in Biotechnology, University of Maryland Biotechnology Institute, 9600 Gudelsky Drive, Rockville, Maryland 20850*

*Received March 5, 1997; Revised Manuscript Received May 21, 1997*[⊗]

ABSTRACT: The role that domain flexibility plays in the enzymatic activity of $\beta$-lactamase from *Staphylococcus aureus* PC1 was investigated by producing two circularly permuted molecules. The C- and N-termini of the wild-type enzyme are adjacent to each other and remote from the active site, which is located between two domains. The polypeptide chain crosses over from one domain to the other twice. For the circularly permuted molecules, the termini were joined by an eight amino acid residue insertion, and new termini were introduced elsewhere. The first construct, termed cp254, was cleaved in a loop remote from the domain interface. The crystal structure of cp254 has been determined and refined at 1.8 Å resolution, revealing essentially the same structure as that of the native protein. The activity profile with a representative sample of $\beta$-lactam antibiotics is also very similar to that of wild-type $\beta$-lactamase. The termini of the second circularly permuted mutant, cp228, occur within the second crossover region and therefore may enhance the flexibility of the molecule. Cp228 $\beta$-lactamase shows a large decrease in enzymatic activity toward the sample of $\beta$-lactam antibiotics, with catalytic rates that are 0.5−1% of those of the wild-type enzyme. One exception is the hydrolysis of the third generation cephalosporin, cefotaxime, which is hydrolyzed by the cp228 enzyme 10-fold faster than by wild-type $\beta$-lactamase. Cp228 has not been crystallized. However, the circular dichroism spectra of the two circularly permuted proteins are very similar, indicating that, by analogy to cp254, cp228 adopts a global folded state. Thermal denaturation experiments reveal that cp254 is somewhat less stable than the wild-type enzyme, whereas cp228 is substantially less stable. Together, the data highlight the profound consequences that introducing flexibility at the domain interface has on both enzyme activity and protein stability.

The class A $\beta$-lactamase (EC 3.5.2.6) from *Staphylococcus aureus* PC1 consists of two closely associated domains, with the active site located at the domain interface (Herzberg & Moult, 1987). One domain contains the 40 N-terminal and 75 C-terminal amino acid residues. These are organized in a three-helix layer packing against one face of a five-stranded antiparallel $\beta$-sheet layer (Figure 1). This fold has been termed an open-face $\beta$-sandwich (Richardson, 1981). Unlike other open-face $\beta$-sandwich proteins, in $\beta$-lactamase the second face of the $\beta$-sheet is not exposed to solvent. Instead, the second domain, comprising the central 145 amino acid residues of the polypeptide chain, folds into an assortment of α-helices that pack against the second face of the $\beta$-sheet. The polypeptide chain crosses over from one domain to the other twice, and each of these crossovers is rather unusual. The first crossover forms an extended chain that traverses the $\beta$-sheet perpendicular to the strands' direction. The following residue is the catalytic serine, Ser70. The second crossover runs along the side of the $\beta$-sheet. It forms a long, rarely observed, left-handed connection between the helical domain and the $\beta$-sheet. Being located at the domain interface, the active site architecture and the enzyme function should depend on the precise conformation and the structural integrity of the crossovers.

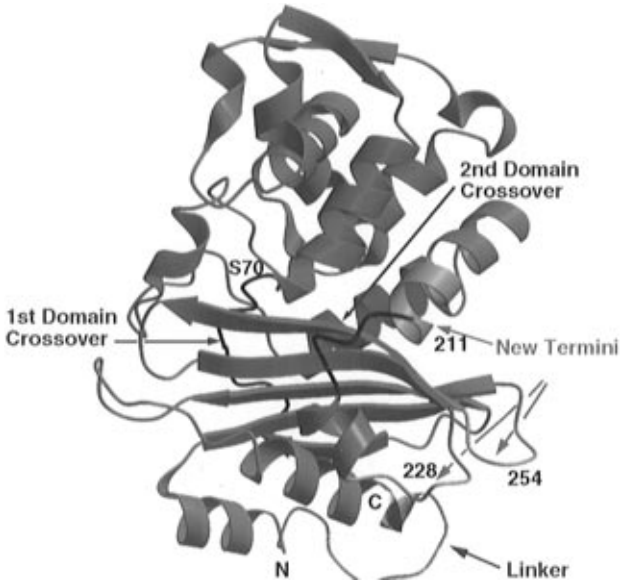


FIGURE 1: Ribbon diagram of $\beta$-lactamase highlighting key positions related to the design of the circularly permuted proteins. N and C correspond to the termini of the native structure. A trace of the designed linker is depicted by a blue dotted line as it is only a model. The positions of introduced new termini are highlighted in yellow and the domain crossovers in red.

One would expect that catalysis and substrate specificity may be modified by enhancing flexibility at the domain interface. This hypothesis may be tested by introducing new C- and N-termini at one of the crossovers, thereby engineering a less tight domain association. While cleaving the chain at the first crossover may have too severe consequences

[†] Supported by NIH Grant RO1-AI27175.

[‡] The coordinates of the crystal structure of cp254 $\beta$-lactamase have been deposited in the Brookhaven Protein Data Bank (entry code 1ALQ).

* To whom correspondence should be addressed (telephone, 301-738-6245; fax, 301-738-6255; E-mail, osnat@carb.nist.gov).

[⊗] Abstract published in *Advance ACS Abstracts,* July 1, 1997.

because of its proximity to the catalytic Ser70, cleavage at the second crossover seems a better choice because it defines part of the domain interface but is not as intimately associated with the active site as the first crossover. Circularly permuted molecules provide the tool to produce proteins with new termini.

In a circularly permuted protein the N- and C-termini of the native molecule have been joined and new termini introduced somewhere else along the polypeptide chain. Bovine pancreatic trypsin inhibitor was the first protein that was permuted in this manner (Goldenberg & Creighton, 1983). With the advent of recombinant DNA technology, numerous other circularly permuted proteins that retain structural integrity and activity have been produced [for a review see Heinemann and Hahn (1995)]. Mostly, the new termini were introduced in solvent-exposed loops. However, recently a method for generating random circular permutations of genes has been applied to aspartate transcarbamoylase, showing that termini can be tolerated also within secondary structure units (Graf & Schachman, 1996). It is not known, though, to what extent such interrupted secondary structure units maintain their fold. The crystal structures of two circularly permuted proteins, $\beta$-glucanase H(A16-M) and $\alpha$-spectrin SH3 domain, have been determined (Hahn et al., 1994; Viguera et al., 1996). These are single-domain all-$\beta$ structures. In both cases there are only minor changes in the three-dimensional structures compared with the native proteins, which are localized in the regions of the new linkers and the new termini.

In the current study, two circularly permuted proteins have been produced, each with an eight residue long peptide that joins the N- and C-terminal helices of the native molecule (Figure 1). One construct is cleaved at the second crossover with the N-terminal residue before position 228. It will be termed cp228 $\beta$-lactamase throughout. The second construct is cleaved in a loop more distant from the domain interface, within the open-face $\beta$-sandwich domain, with the N-terminal residue at position 254. This molecule will be termed cp254 $\beta$-lactamase. The structural and functional consequences of these manipulations are described.

## MATERIALS AND METHODS

*Bacterial Strains, Plasmids, and DNA Manipulations.* *Escherichia coli* TG1, which was used as a host for genetic manipulations and protein expression, was provided by Dr. P. Bryan (Center for Advanced Research in Biotechnology, Rockville, MD). The previously described vector pTS32 (Zawadzke et al., 1995), including the gene that encodes the *S. aureus* $\beta$-lactamase PC1, served as the starting point for the construction of the cp228 and cp254 $\beta$-lactamases. The gene was further modified using polymerase-catalyzed chain reaction (PCR) (Saiki et al., 1988). The sequence between the Shine−Dalgarno site and the initiating methionine has been altered, and new restriction sites have been introduced. The resulting vector pKH1 includes a *Xho*I restriction site immediately following the C-terminal stop codon of the $\beta$-lactamase gene and the following sequence preceding the initiating ATG:

```
MfeI        SD      KpnI  Met

CAATTGCACACAGGAGATGGTACCATG
```

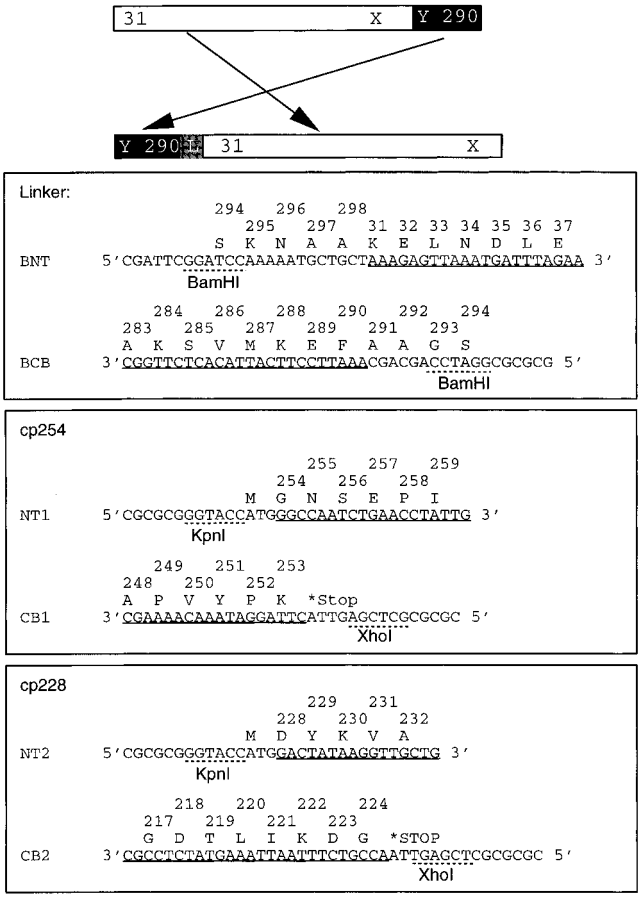


FIGURE 2: Scheme of the construction of the circularly permuted genes of $\beta$-lactamase. The native protein spans residues 31−290. X and Y denote the protein segments whose order has been interchanged in the circularly permuted genes. L denotes the insertion of the linker peptide. A list of the primers used is provided.

Restriction enzymes, T4 DNA ligase, and Vent polymerase were obtained from New England Biolabs (Beverly, MA). Oligonucleotides were synthesized on an Applied Biosystems 380B DNA synthesizer. Chloramphenicol, for selection of plasmid-containing bacteria, was used at a final concentration of 20 $\mu$g/mL. It was purchased from Sigma Chemical Co. (St. Louis, MO). IPTG was obtained from Gold Biotechnology (St. Louis, MO). General methods for purification, restriction, and modification of plasmid DNA were performed as described by Maniatis et al. (1982). DNA fragments excised from agarose gels were purified using the QuiaxII Kit (Quiagen, Hilden, Germany). PCR was performed using the Gene Amp kit available from Perkin-Elmer Cetus (Norwalk, CT). Approximately 0.5 $\mu$g of template DNA and 5 pmol of each primer were used in each PCR; dNTPs, buffer, and magnesium chloride were included as recommended by the kit's manufacturer. Twenty-five cycles of amplification were carried out with the following temperatures: 1 min at 72 °C, 1 min at 92 °C, and 1 min at 52 °C. Finally, the ragged ends were filled at 72 °C for 8 min.

Figure 2 shows the primers used for constructing the circularly permuted genes. For each of the permutations two PCR reactions with the plasmid pHK1 including wild-type $\beta$-lactamase as the template were carried out. The primers BNT and CB1 for cp254 or BNT and CB2 for cp228 were used to construct the new C-terminal fragment of the gene, including the coding nucleotides for five linker residues 294−

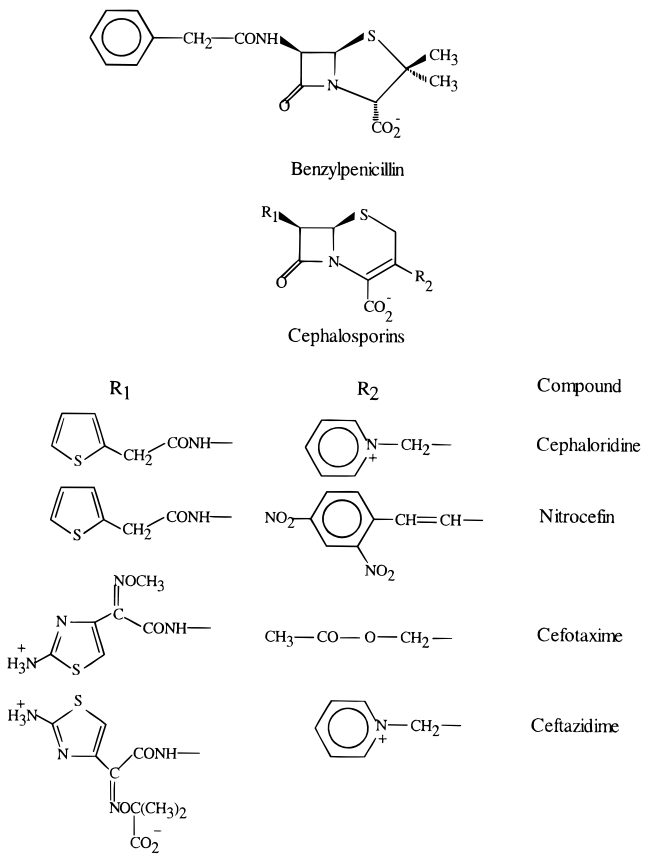


FIGURE 3: Scheme of the $\beta$-lactam antibiotics selected for this study.

298 and a *Bam*HI restriction site at the first linker residue, 294. The primers NT1 and BCB for cp254 or NT2 and BCB for cp228 were used to construct the new N-terminal fragment of the gene with the encoding of four linker residues, 291−294 and a *Bam*HI restriction site at 293 and 294 of the primer BCB.

The resulting DNA fragments were purified by electrophoresis on agarose gels and digested with the restriction endonuclease *Bam*HI. The two gene fragments were ligated together using T4 DNA ligase, and the ligation mixture, now including the complete circularly permuted gene, was used as the template for a third PCR reaction (primers NT1/CB1 or NT2/CB2 for cp254 and cp228, respectively) with the same PCR program as before. The products were purified on an agarose gel. The genes were digested with *Kpn*I and *Xho*I, ligated into the vector pKH1, and transformed into *E. coli* TG1 cells. The correct amino acid sequences were confirmed by the method of Sanger et al. (1997).

*Protein Expression and Purification.* Cp254 and cp228 $\beta$-lactamases were expressed in *E. coli* at approximately 2-fold and 8-fold reduced levels compared with wild-type $\beta$-lactamase, yielding 4 and 1 mg of protein/L of medium, respectively. The protein purification procedure was as previously published (Zawadzke et al., 1995), except that, to prevent proteolytic degradation, phenylmethanesulfonyl fluoride inhibitor was added to the lysed cells.

*Enzyme Kinetics.* The chromogenic cephalosporin, nitrocefin, was obtained from Unipath (Ogdensburg, NY); other $\beta$-lactam compounds used for kinetic characterization were purchased from Sigma. The chemical schemes of the antibiotics used in this study are shown in Figure 3. Kinetic measurements were made on a Hewlett-Packard 8452A diode array spectrophotometer. All assays were performed at 25 °C in 0.1 M potassium phosphate buffer at pH 6.8. Substrate hydrolysis was monitored by loss of UV absorption for benzylpenicillin ($\Delta\epsilon_{232} = 940$ M$^{-1}$ cm$^{-1}$), cephaloridine ($\Delta\epsilon_{260} = 10\,700$ M$^{-1}$ cm$^{-1}$), cefotaxime ($\Delta\epsilon_{262} = 7250$ M$^{-1}$ cm$^{-1}$), and ceftazidime ($\Delta\epsilon_{260} = 10\,200$ M$^{-1}$ cm$^{-1}$) and by the increase in absorbance at 500 nm for nitrocefin ($\Delta\epsilon_{500} = 15\,900$ M$^{-1}$ cm$^{-1}$).

Substrate-induced progressive inactivation was analyzed by fitting the progress curves to the general integrated equation (Waley, 1991; Zawadzke et al., 1995):

$$P = v_s t - (v_s - v_i)(1 - e^{-kt})/k \quad (1)$$

where $P$ is the product to enzyme molar ratio, $v_s$ is the steady-state velocity or $k_{cat}$, $v_i$ is the initial velocity, and $k$ is the rate of change from $v_i$ to $v_s$ or burst rate constant.

*Crystallization.* Crystals of cp254 $\beta$-lactamase were obtained at room temperature by the hanging drop method. The drops contained 2.5 $\mu$L protein (10 mg/mL of protein in 60% saturated ammonium sulfate buffered by 10 mM potassium phosphate at pH 6.8) and 2.5 $\mu$L of reservoir solution [70% saturated ammonium sulfate, 0.3 M KCl, 100 mM $NaHCO_3$ buffer at pH 8.0, 0.5% v/v poly(ethylene glycol) 600]. Crystals appeared overnight. They were orthorhombic, belonging to the space group $I222$ with cell dimensions $a = 53.9$ Å, $b = 94.2$ Å, and $c = 138.3$ Å. The cell parameters are similar to those of the crystals of native $\beta$-lactamase ($a = 53.9$ Å, $b = 94.0$ Å, $c = 139.1$ Å). Crystallization attempts of cp228 $\beta$-lactamase were unsuccessful.

*Data Collection.* X-ray diffraction data were collected on a Siemens multiwire area detector mounted on a Siemens three-axis goniostat using a single crystal of cp254 $\beta$-lactamase of approximate dimensions of $0.4 \times 0.4 \times 0.6$ mm$^3$. Graphite monochromated Cu K$\alpha$ radiation was generated with a Rigaku Rotaflex RU-200BH rotating anode. The data were processed with the computer program suite XENGEN (Howard et al., 1987). Data to 1.8 Å resolution were collected at room temperature. Data processing statistics are summarized in Table 1.

Table 1: Data Processing Statistics for Cp254 $\beta$-Lactamase

| shell lower limit (Å) | no. of reflections collected | no. of reflections missing | no. of observations | $\langle I/\sigma(I)\rangle$ | $R_{merge}$[a] |
|---|---|---|---|---|---|
| 3.27 | 5711 | 29 | 43 361 | 61.9 | 0.048 |
| 2.60 | 5432 | 111 | 33 400 | 25.2 | 0.083 |
| 2.27 | 5113 | 373 | 27 842 | 12.1 | 0.152 |
| 2.06 | 4879 | 608 | 21 668 | 6.6 | 0.226 |
| 1.91 | 4596 | 830 | 12 468 | 3.5 | 0.286 |
| 1.80 | 4082 | 1369 | 8 796 | 1.8 | 0.408 |
| total | 29813 | 3320 | 147 535 | 20.4 | 0.079 |

[a] $R_{merge} = \sum_h\sum_i|\langle I(h)\rangle - I(h)_i|/\sum_h\sum_i I(h)_i$ for equivalent reflections.

*Structure Determination and Refinement.* Structure factors were calculated using the protein coordinates of the native structure (Herzberg, 1991; entry code 3BLM in the Protein Data Bank) and initially omitting residues 31−34, 252−256, and 288−290 from the model. The solvent molecules of 3BLM were also omitted. The initial $R$-factor was 0.293 ($R = \sum_h||F_o| - |F_c||/\sum_h|F_o|$, where $|F_o|$ and $|F_c|$ are the observed and calculated structure factor amplitudes, respectively) for data in the resolution range 7.0−1.9 Å for which $F \geq 2\sigma(F)$. Several cycles of positional refinement followed

by displacement parameter refinement were carried out with X-PLOR (Brünger, 1992a). Difference electron density maps with the coefficients $2F_o - F_c$ and $F_o - F_c$ and calculated phases were inspected on an INDIGO2 interactive graphics system using the program Turbo-Frodo (Roussel & Cambillau, 1989). As density corresponding to missing amino acid residues became apparent, these were added to the model. The progress of the refinement was monitored by calculating a free *R*-factor, $R_{free}$, for 10% of the structure factors which were not included in the refinement (Brünger, 1992b). At $R = 0.189$ and $R_{free} = 0.241$, the refinement was continued with the program SHELXL-96 (Sheldrick, 1996). All measured data up to 1.8 Å resolution were included except for the 10% of the reflections that were used for $R_{free}$ calculations. The structure was refined against $F^2$, minimizing a weighted *R* on $F^2$:

$$R(F^2) = [\sum_h [w(F_o^2 - F_c^2)^2] / \sum_h [w(F_o^2)^2]]^{0.5}$$

where $w = 1/[\sigma^2(F_o^2) + (0.1P)^2 + 0.2P]$ and $P = [\max(F_o^2,0) + F_c^2]/3$.

The solvent structure was optimized automatically by iterative placement of water molecules at positive peaks identified by difference Fourier synthesis, employing distance criteria of ≥2.4 Å from hydrogen bond donors or acceptors. The validity of the assignment was confirmed by inspection of the electron density maps. Some water molecules that did not initially fulfill the automatic selection criteria but were associated with well-defined density were added to the model. Such cases involved water molecules that later were found to be bridged to the protein by intervening water molecules. Refinement and verification of the water molecules with SHELXWAT followed a protocol in which the occupancies of water molecules with displacement parameters above 60 Å$^2$ were halved during subsequent refinement cycles. Those water molecules whose displacement parameters still refined to values above 60 Å$^2$ after the occupancies were halved were deleted from the model. The validity of water molecules was further confirmed by inspection of the $2F_o - F_c$ electron density map. Diffuse solvent was modeled according to Moews and Kretsinger (1975). Hydrogen atoms were included in the refinement with constrained geometry and displacement parameters. At the end of the process, all data, including the structure factors that were reserved for $R_{free}$ calculation, were refined. Finally ten cycles of full-matrix least-squares refinement were performed.

*Circular Dichroism.* Circular dichroism (CD) spectra were measured with a Jasco 720 spectropolarimeter using a water-jacketed cylindrical cell with a path length of 1.0 mm. Temperature control was provided by a Neslab RTE-110 circulating water bath interfaced with a MTP-6 temperature programmer. All experiments were carried out with 22 $\mu$M protein solutions containing 0.8 M ammonium sulfate and 10 mM potassium phosphate buffer at pH 6.8. The ammonium sulfate enhances the protein stability and protects it from proteolytic degradation (Banerjee et al., 1997). Far-UV CD spectra of the circular permuted $\beta$-lactamases were scanned between 200 and 250 nm at 25 °C. Three scans were averaged. Unfolding transitions were monitored at 220 nm, varying the temperature from 0 to 90 °C at a rate of 1 °C/min. After reaching 90 °C the system was cooled to 25 °C, and the spectra were measured again to assess whether refolding occurred. As discussed below, unfolding was irreversible by this criterion.

## RESULTS AND DISCUSSION

*Design of the Circularly Permuted Proteins.* Of the two circularly permuted $\beta$-lactamases that were produced, the N- and C-termini of one are located in a region remote from the domain interface and not within the domain crossovers (cp254). The termini of the second protein (cp228) reside on the second domain crossover (Figure 1). The gene for a third circularly permuted molecule was also produced. Its N-terminus was at position 211 (cp211), at the end of the helix preceding the second domain crossover. However, the expression level of this construct was low, although a visual nitrocefin assay of the lysed cell, assessed by a color change, confirmed that they contained active $\beta$-lactamase. Deletion of residue 210 or of the three residues 208−210, to allow for a gap between the new N- and C-termini, did not improve the level of protein expression. The reason for the low expression level is unclear. Possibly, the protein suffered proteolytic degradation in the cell or the transcription or translation rates were diminished because of unfavorable codon usage or particular RNA structure.

Further studies were carried out with the two designed circularly permuted proteins that could be overexpressed successfully. Their termini are in regions that are not involved in crystal packing interactions within the context of the native crystal form, so that in principle the proteins could be crystallized isomorphously with the native crystals. Moreover, residues 228 and 254 in the native crystal reside on structural segments that exhibit the highest main-chain crystallographic temperature factors (Herzberg, 1991). Thus, it was reasonable to assume that modification of such flexible segments would not be detrimental to the overall fold. These considerations led to the successful crystallization of cp254.

The cleavage between Lys253 and Gly254 in cp254 is in a loop connecting two $\beta$-strands, within the five-stranded $\beta$-sheet. As this is a mobile and solvated region, the addition of a methionine in front of Gly254 for initiation of translation should not interfere with folding. The design of the termini of cp228 raised an additional concern because of the unusual left-handed turn of the crossover whose significance is not understood. Also, it was not obvious that a simple cleavage point would suffice to accommodate minor structural changes that are expected to occur when the chain is interrupted and an initiator methionine is inserted. To provide enough space for structural adjustments, three amino acid residues, 225−227, were deleted.

The chain termini of native $\beta$-lactamase reside on two adjacent helices with the N- and C-terminal residues approximately 13 Å apart. For the circularly permuted molecules, the peptide that joins the termini was designed by searching the Protein Data Bank for pairs of helices in mixed $\alpha,\beta$ proteins with spatial dispositions similar to those of the C- and N-terminal helices in $\beta$-lactamase. The linker between a pair of helices in glucose oxidase (PDB entry code 1GAL; Hecht et al., 1993) fitted quite well. An eight-residue insertion incorporated into the circularly permuted genes was intended to mimic the conformation of the connecting loop in glucose oxidase and to extend the N-terminal helix of the native molecule by half a turn by analogy to glucose oxidase. Amino acid residues of high helical propensity were chosen

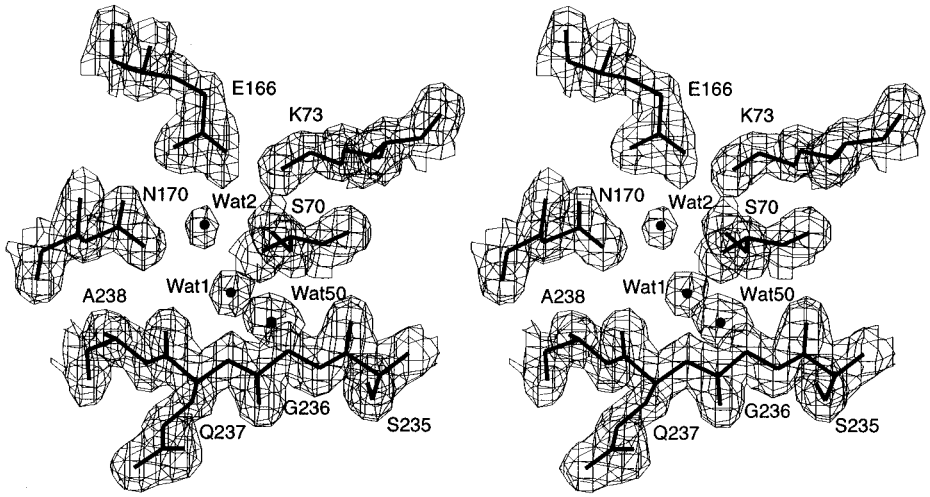


FIGURE 4: Stereoscopic representation of the electron density map in the region of the active site, displayed with the protein model. The map is calculated with the coefficient $2F_o - F_c$ and contoured at the $1.2\sigma$ level. Wat denotes water molecules.

for this. The sequence was further modified to avoid short contacts between side chains of the inserted segment and the rest of the $\beta$-lactamase molecule and to introduce a *Bam*HI restriction site in the middle of the linker. The sequence of the eight-residue linker peptide is

Ala-Ala-Gly-Ser-Lys-Asn-Ala-Ala

Note that the consensus numbering scheme of native $\beta$-lactamase (Ambler et al., 1991) is used throughout. In this scheme, the mature native $\beta$-lactamase molecule spans residues 31−290 (residues 1−30 comprise a signal peptide that is cleaved from the excreted protein and have not been included in the genetically engineered protein). The linker peptide of the circularly permuted molecule is numbered 291−298.

Inspection of the crystal environment of native $\beta$-lactamase indicated that the linker could be accommodated without perturbing crystal packing.

*Crystal Structure of Cp254* $\beta$-Lactamase. The model of cp254 $\beta$-lactamase consists of amino acid residues 256−290, four of the eight linker residues (numbered 291, 292, 297, and 298) and residues 31−253. No electron density is associated with the initiator methionine, with the first two amino acid residues, 254−255, and with four residues of the linker, 293−296. These are not included in the model. Moreover, the displacement parameters of the four linker residues that could be modeled are quite high. In addition, residues 226−230 also refined with high displacement parameters. There is no electron density associated with the side chain of Lys227, and the corresponding atoms are not included in the model. The model contains 212 water molecules, 1 sulfate ion, and 1 carbonate ion.

The conventional *R*-factor on *F* is 0.156 ($R_{free} = 0.215$) for data between 30 and 1.8 Å resolution for which $F > 4\sigma(F)$ and 0.196 for all measured data ($R_{free} = 0.256$). The $R(F^2)$ value is 0.360 for all measured data. The root mean square (rms) deviations from ideal bond length and bond angle values of the standard geometry as compiled by Engh and Huber (1991) are 0.020 and 0.040 Å, respectively. The electron density map at the active site region is shown in Figure 4.

Two non-glycine residues, Asp69 and Leu220, have sterically strained main-chain dihedral angles, consistent with their conformation in the native structure. A non-proline *cis* peptide bond is observed between Glu166 and Ile167, as previously identified in native $\beta$-lactamase (Herzberg, 1991).

Within the accuracy of the structure determination, the structure of cp254 $\beta$-lactamase is almost identical to that of the parent molecule. Superposition of the native and mutant models yields a rms difference of 0.2 Å for the α-carbon atoms and 0.7 Å for all atoms (Figure 5). The largest differences occur in the regions of the new N- and C-termini (Figure 6). Residues 226−228 on the domain crossover are adjacent to the new termini. These too refined with elevated displacement parameters when compared to the native structure, indicating greater flexibility, although they are clearly identified in the electron density map. The regions of enhanced flexibility did not affect the active site, which remained indistinguishable from that of native $\beta$-lactamase. The conformations of those linker residues that were identified in the electron density map are different from the conformations of the corresponding residues in the model that was developed during the design step. In particular, the N-terminal helix in the native structure is not extended in the engineered protein as planned. Instead, the helix is broken at residue 31 as it is in native $\beta$-lactamase.

The water structure of cp254 is also quite similar to that assigned to the native $\beta$-lactamase crystal structure. Although the assignment of the water molecules was performed independently of the water structure in native $\beta$-lactamase, and despite the different refinement programs employed, 85 (41%) of the water molecules in cp254 are located within 0.5 Å of water molecules in native $\beta$-lactamase, and 130 (61%) water molecules are located within 1.0 Å of water molecules in the native structure. The water molecule assigned the role of deacylation, the water molecule in the oxyanion hole, and the internal water molecules (Herzberg, 1991) were all identified in cp254.

One charge−charge interaction has changed at Lys215. The intermolecular salt bridge between Lys215 and Glu124 in the native structure is replaced by an intramolecular salt bridge between Lys215 and Asp218 in cp254. The side chain of Lys215 refined with high displacement parameters in both the native and cp254 molecules, whereas the carboxylate-containing side chain in each case exhibits low displacement parameters. This indicates that the side chain

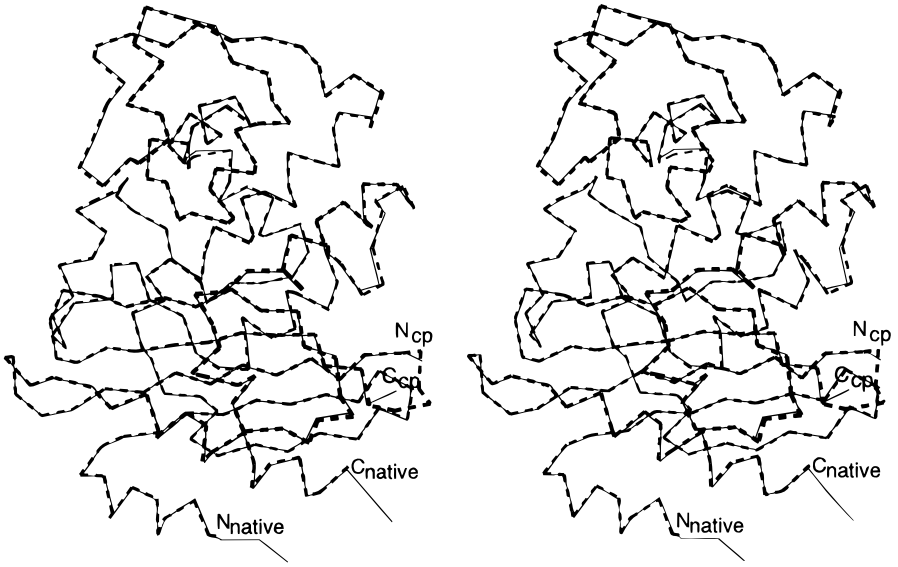


FIGURE 5: Stereoscopic representation of the superposition of native $\beta$-lactamase and cp254. Virtual bonds between α-carbon atoms of the native structure are shown in broken lines, and those of cp254 are shown in continuous lines.

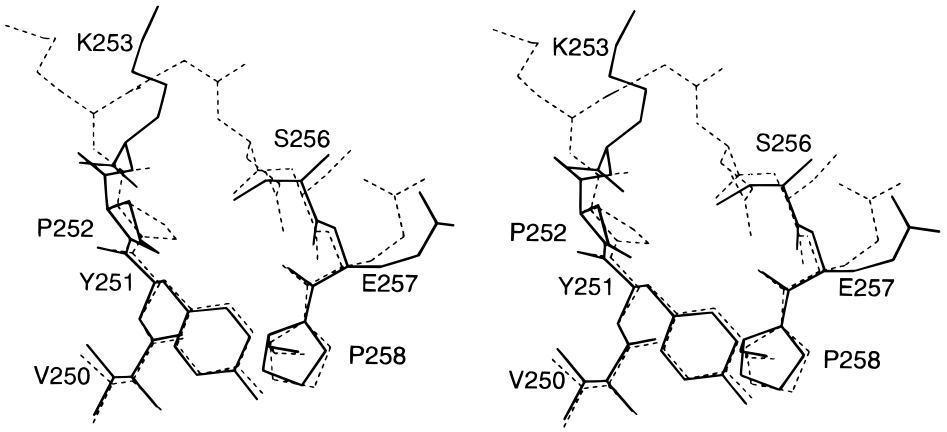


FIGURE 6: Stereoscopic representation of the N- and C-termini of cp254 $\beta$-lactamase superpositioned on the corresponding region of the native structure. Bonds of the cp254 molecule are shown in continuous lines and of the native molecule in broken lines.

of Lys215 can adopt two alternative conformations that give rise to the two types of salt bridge. A few more side chains of solvated lysine residues adopt alternative conformations when compared with the native structure. The hydrogen bond pattern remains invariant, except for the obvious changes at the old and new terminal regions.

Two anions have been identified in the electron density map of the cp254 $\beta$-lactamase crystal: a sulfate and a carbonate. The sulfate ion is located in a position that is modeled as a water molecule in the native structure. The carbonate displaces a lysine side chain. The electrostatic environment around each position is consistent with the occupancy of an anion. Presumably, the 1.8 Å data of the cp254 crystal compared with the lower resolution 2.0 Å data of native $\beta$-lactamase gave rise to a higher quality electron density map that enabled the identification of the ions.

*Structural Information by CD.* Since cp228 $\beta$-lactamase failed to crystallize, far-UV CD was employed to provide some structural information about this molecule (Figure 7). By CD, cp228 $\beta$-lactamase exhibits a similar amount of secondary structure as that of cp254 $\beta$-lactamase whose crystal structure has been determined, and the CD signal of both is slightly lower than that of the wild-type protein. Together, the data indicate that cp228 adopts a global fold comparable with that of cp254.

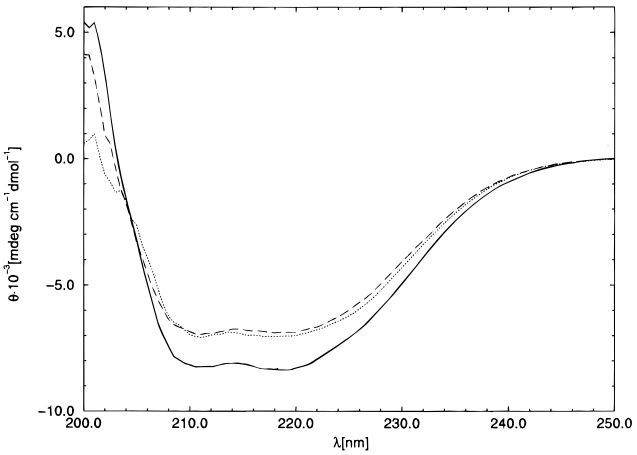


FIGURE 7: Far-UV circular dichroism spectra of wild-type (solid line), cp228 (dotted line), and cp254 (dashed line) $\beta$-lactamases at 25 °C. For each, the mean residue ellipticity is plotted as a function of wavelength. The concentration of each protein was 22 $\mu$M, and the solutions contained 0.8 M saturated ammonium sulfate and 0.1 M potassium phosphate at pH 6.8.

As with wild-type $\beta$-lactamase from *S. aureus* PC1 (Rahil & Pratt, 1994; Banerjee et al., 1997), the thermal denaturation of either circularly permuted proteins is irreversible. This is not unusual for protein molecules. Manly et al. (1985)

Table 2: Kinetic Data[a] for the Wild-Type and Circularly Permuted $\beta$-Lactamases

| compound | parameter | wild type | cp254 | cp228 |
|---|---|---|---|---|
| benzylpenicillin | $k_{cat}$ | 141 | 118 | 0.468 |
| | $K_m$ | 3 | 11 | 87 |
| nitrocefin | $k_{cat}$ | 14.0 | 12.2 | 0.1197 |
| | $K_m$ | 1 | 2 | 12 |
| cephaloridine | $v_i$ | 1.3 | 2.6 | 0.0088 ($k_{cat}$) |
| | $v_s$ | 0.077 | 0.054 | —[b] |
| | $k$ | 0.080 | 0.081 | —[b] |
| | $K_m$ | <1 | <1 | 15 |
| cefotaxime | $k_{cat}$ | 0.0006 | 0.0007 | 0.0054 |
| ceftazidime | $k_{cat}$ | ND[c] | ND[c] | ND[c] |

[a] Velocities are expressed in $s^{-1}$, and $K_m$ values are expressed in $\mu$M. [b] The progress curve is linear. [c] ND = no detectable hydrolysis.

have shown that if a two-state thermodynamic model can be applied to the unfolding process and the van't Hoff equation is obeyed, the transition may be viewed as fundamentally reversible. Following the same rational, Rahil and Pratt (1994) found that the thermal unfolding of $\beta$-lactamase from *S. aureus* PC1 is reversible prior to the onset of aggregation. Hence, the transition temperature, $T_m$, reflects protein stability.

The unfolding process of the wild-type protein has been followed in the presence of 0.8 M ammonium sulfate and shown to fit a two-state transition with a $T_m$ of 74 °C (Banerjee et al., 1997). For comparison with the wild-type $\beta$-lactamase, the unfolding experiments of the circularly permuted proteins were performed in the same ammonium sulfate concentration. The unfolding of cp254 spans a wider temperature range (20 °C) compared with the wild-type enzyme, with a $T_m$ of 71 °C. The temperature range for the unfolding of cp228 is even broader, starting at 50 °C and spanning 35 °C. Because of evidence of aggregation during the denaturation process, the data were not interpreted further. Nevertheless, it is clear that the two circularly permuted proteins are less stable than the wild-type $\beta$-lactamase, with cp228 the least stable.

*Enzymatic Activity.* Both cp228 and cp254 $\beta$-lactamases are enzymatically active, but the kinetics of each of these circularly permuted molecules is quite different (Table 2). The substrate profile of cp254 $\beta$-lactamase is very similar to that of wild-type $\beta$-lactamase: (a) Benzylpenicillin and nitrocefin are hydrolyzed at essentially the same rates by both wild-type and cp254 enzymes. (b) With cephaloridine, the two $\beta$-lactamases exhibit substrate-induced progressive inactivation, although the initial velocity is 2-fold higher for cp254. (c) As with the wild-type enzyme (Zawadzke et al., 1996), hydrolysis of the third generation cephalosporin, cefotaxime, is extremely slow, and that of ceftazidime is undetectable under the experimental conditions. The kinetic results are consistent with the close structural similarity between the cp254 and the native enzymes. A previous study of a circularly permuted *Bacillus* $\beta$-glucanase H(A16-M), whose active site is located remotely from both the new termini and the linker region, arrived at the same conclusion that the enzymatic activity of the circularly permuted molecule resembled that of the wild-type enzyme (Hahn et al., 1994).

In contrast to cp254 $\beta$-lactamase, the enzymatic activity of cp228 $\beta$-lactamase is much altered compared with the wild-type enzyme (Table 2). The $k_{cat}$ values are reduced by approximately 300-fold for benzylpenicillin and by 100-fold for nitrocefin and cephaloridine. Surprisingly, the hydrolysis of the third generation cephalosporin, cefotaxime, progresses at a 10 times higher rate than the rate observed with the wild-type $\beta$-lactamase. However, no enzymatic activity was detected toward another third generation cephalosporin, ceftazidime, a compound with a bulkier side-chain substituent compared with that of cefotaxime.

*Origin of Altered Enzyme Stability and Activity.* The reduced thermal stability of cp254 compared with the stability of wild-type $\beta$-lactamase is attributed to imperfection in the design of the linker peptide and to the choice of the position of the new termini, because these are the only features in the crystal structure that differ between the two structures. Lower stability (assessed by urea denaturation experiments) compared with the wild-type protein was also measured for the circularly permuted α-spectrin SH3 domain (termed N47-D48S) whose crystal structure resembles closely that of the wild-type protein (Viguera et al., 1995, 1996). With the structure of cp254 at hand, a second generation of a circularly permuted $\beta$-lactamase could be engineered to achieve higher stability by seeking to enhance the number of hydrophobic and electrostatic interactions between the linker and the remaining molecule. A similar approach may be applied to improving contacts at the termini positions.

As there is no detailed structural information about cp228 $\beta$-lactamase, one may only speculate that interrupting the polypeptide chain at the domain crossover weakens the association between the two domains. The region of interruption exhibits high crystallographic temperature factors in the native structure. Cp228 is expected to have an increased mobility because of the chain discontinuity, a mobility that could propagate toward the domain interface, hence the observed reduction in the stability of the molecule and the cooperativity of the unfolding process.

The reduced enzymatic activity of cp228 is also attributed to the breaking of the polypeptide chain at the domain crossover, which may perturb the domain association and thus alter the positioning of the catalytic apparatus. Although in this case the rates of hydrolysis of most substrates that have been examined are reduced, the hydrolysis rate of cefotaxime is actually increased by 10-fold when compared with that of the wild-type $\beta$-lactamase. Acquired new substrate specificity in $\beta$-lactamases is a subject of much research, as it pertains to drug resistance problems. Variant enzymes that can hydrolyze a new class of $\beta$-lactam antibiotics, for example, third generation cephalosporins, have been interpreted in terms of the effect of specific active site mutations. In previous work, the acquired resistance to the third generation cephalosporins conferred by an engineered $\beta$-lactamase from *S. aureus* PC1 was correlated with structural changes determined by X-ray crystallography (Zawadzke et al., 1996). The A238S·I239del mutations induced a shift in a $\beta$-strand that forms part of the active site, leading to the opening of the active site gully where the bulky side-chain substituent of the third generation cephalosporins should be accommodated. The current work indicates that broader substrate specificity in $\beta$-lactamase may arise not only by amino acid replacements in the active site but also by altered interdomain association and flexibility. Presumably, the new flexibility enables adjustments within the active site and accommodation of the bulky side-chain substituent of the cefotaxime. With cp228, however, the effect is only marginal, as evident by the low hydrolysis rate

of cefotaxime and the inability of the enzyme to hydrolyze ceftazidime, a compound with an even bulkier side-chain substituent.

*Relation to Other Crystal Structures of Circularly Permuted Proteins.* Despite the many reports of circularly permuted proteins (Heinemann & Hahn, 1995), this is only the third example of a crystal structure determination of such a protein. The other structures are of $\beta$-glucanase H(A16-M) (Hahn et al., 1994) and of $\alpha$-spectrin SH3 domain (Vigura et al., 1996). Both proteins adopt a single-domain $\beta$-sandwich fold, with the N- and C-termini located on adjacent $\beta$-strands. The $\beta$-gluconase termini were directly linked to each other, while those of $\alpha$-spectrin SH3 domain were linked by a two-residue insertion. $\beta$-Structures can be readily connected in this manner to form a hairpin loop. In contrast, the N- and C-terminal structural units of $\beta$-lactamase are helices, requiring a longer peptide insertion to link them. Our design strategy differed from those previously reported [reviewed by Heinemann and Hahn (1995)], which included several glycine residues to assure linker flexibility. The goal of the current study was to avoid introduction of high mobility in the rather long linker peptide because of the concern that it could induce long-range disorder of the adjacent helical units. This in turn could alter the structure beyond the intended perturbation at the new termini, which would complicate the interpretation and prevent evaluation of the hypothesis that flexibility at the domain interface impacts function. The crystal structure confirms that there is no long-range disorder and the helices are as well-defined as in native $\beta$-lactamase, even though the linker peptide itself is partially disordered.

## ACKNOWLEDGMENT

We thank Celia Chen for help with DNA sequencing and Lan Wang for help with the CD experiments. We are grateful to Soojay Banerjee, Philip Bryan, William dall'Acqua, Marina Lebedeva, and John Moult for helpful discussions.

## REFERENCES

Ambler, R. P., Coulson, A. F. W., Frère, J.-M., Ghuysen, J.-M., Joris, B., Forsman, M., Levesque, R. C., Tiraby, G., & Waley, S. G. (1991) *Biochem. J. 276*, 269−270.

Banerjee, S., Shigematsu, N., Pannell, L. K., Ruvinov, S., Orban, J., Schwarz, F., & Herzberg, O. (1997) *Biochemistry* (submitted for publication).

Brünger, A. T. (1992a) *X-PLOR version 3.1, a system for x-ray crystallography and NMR*, Yale University Press, New Haven and London.

Brünger, A. T. (1992b) *Nature 355*, 472−475.

Engh, R. A., & Huber, R. (1991) *Acta Crystallogr. A47*, 392−400.

Goldenberg, D. P., & Creighton, T. E. (1983) *J. Mol. Biol. 165*, 407−413.

Graf, R., & Schachmann, H. K. (1996) *Proc. Natl. Acad. Sci. U.S.A. 93*, 11591−11596.

Hahn, M., Piotukh, K., Borriss, R., & Heinemann, U. (1994) *Proc. Natl. Acad. Sci. U.S.A. 91*, 10417−10421.

Hecht, H. J., Kalisz, H. M., Hendle, J., Schmid, R. D., & Schomburg, D. (1993) *J. Mol. Biol. 229*, 153−172.

Heinemann, U., & Hahn, M. (1995) *Prog. Biophys. Mol. Biol. 64*, 121−143.

Herzberg, O. (1991) *J. Mol. Biol. 217*, 701−719.

Herzberg, O., & Moult, J. (1987) *Science 236*, 694−701.

Howard, A. J., Gilliland, G. L., Finzel, B. C., Poulos, T., Ohlendorf, D. O., & Salemme, F. R. (1987) *J. Appl. Crystallogr. 20*, 383−387.

Maniatis, T., Fritsch, E. F., & Sambrook, J. (1982) *Molecular cloning: a laboratory approach*, Cold Spring Harbor Laboratory Press, Cold Spring Harbor, NY.

Manly, S. P., Matthews, K. S., & Sturtevant, J. M (1985) *Biochemistry 24*, 3843−3846.

Moews, R. H., & Kretsinger, R. H. (1975) *J. Mol. Biol. 91*, 201−224.

Rahil, J., & Pratt, R. F. (1994) *Biochemistry 33*, 116−125.

Richardson, J. (1981) *Adv. Protein Chem. 34*, 167−339.

Roussel, A., & Cambillau, C. (1989) TURBO-FRODO, in *Silicon Graphics Geometry Partners Directory* (Silicon Graphics, Ed.) pp 77−78, Silicon Graphics, Mountain View, CA.

Saiki, R. K., Gelfand, D. H., Stoffel, S., Scharff, S. J., Higuchi, R., Horn, G. T., Mullis, K. B., & Erlich H. A. (1988) *Science 239*, 487−491.

Sanger, F., Nicklen, S., & Coulson, A. R. (1977) *Proc. Natl. Acad. Sci. U.S.A. 74*, 5463−5467.

Sheldrick, G. M. (1996) *SHELXL-96, a program for crystal structure refinement*, Version $\beta$-test 03, Göttingen.

Viguera, A. R., Blanco, F. J., & Serrano, L. (1995) *J. Mol. Biol. 247*, 670−681.

Viguera, A. R., Serrano, L., & Wilmanns, M. (1996) *Nat. Struct. Biol. 3*, 874−880.

Waley, S. G. (1991) *Biochem. J. 279*, 87−94.

Zawadzke, L. E., Smith, T. J., & Herzberg, O. (1995) *Protein Eng. 8*, 1275−1285.

BI9705117